Pharm Res (2011) 28:1931–1938
DOI 10.1007/s11095-011-0420-y

RESEARCH PAPER

Investigation of the Pharmacokinetics of Romiplostim in Rodents with a Focus on the Clearance Mechanism

Yow-Ming C. Wang • Bethlyn Sloey • Teresa Wong • Prerna Khandelwal • Rebeca Melara • Yu-Nien Sun

Received: 21 December 2010 / Accepted: 4 March 2011 / Published online: 8 April 2011
© Springer Science+Business Media, LLC 2011

ABSTRACT

Purpose Romiplostim, a treatment for adults with immune thrombocytopenia (ITP), is a novel thrombopoietin mimetic agent with a similar mechanism of action as thrombopoietin with no sequence homology. Structurally, it is a peptibody containing thrombopoietin mimetic peptides and the Fc portion of human IgG_1. We investigated romiplostim pharmacokinetics in rodents with a focus on the clearance mechanism.

Methods Studies with appropriate controls were conducted in four models: FcRn knockout mice, thrombocytopenic mice, splenectomized rats, and bilateral nephrectomized rats. Catabolic breakdown of romiplostim was investigated in normal rats. The primary analytical method determines the intact/active romiplostim concentration, and the secondary method determines the sum of romiplostim and its catabolic degradants.

Results FcRn interaction results in prolonged exposure. Platelets are involved in the target-mediated elimination, a saturable process and more prominent at low dose. Splenectomy does not affect the romiplostim pharmacokinetics in rats, an observation not unexpected. Nephrectomy in rats results in a greater increase of romiplostim exposure at a higher romiplostim dose, a nonlinearity likely due to saturation of competing pathway. Catabolism plays a major role in romiplostim elimination.

Conclusion Romiplostim clearance involves multiple mechanisms, including a nonlinear pathway. Consequently, the relative contribution of different mechanisms appears to be dose dependent.

Y.-M. C. Wang (✉) · B. Sloey · T. Wong · P. Khandelwal · R. Melara · Y.-N. Sun
Pharmacokinetics and Drug Metabolism Department, Amgen Inc.
One Amgen Center Drive, 28-3-B
Thousand Oaks, California 91320, USA
e-mail: wang.yowming@gmail.com

KEY WORDS clearance mechanism · nonlinear pathway · pharmacokinetics · rodents · romiplostim

INTRODUCTION

Thrombopoietin (TPO) is the primary physiological regulator of platelet production (1). TPO is the ligand of the cytokine receptor c-Mpl which is expressed on the surface of hematopoietic cells of thrombopoietic lineage, such as megakaryocytes, megakaryocyte progenitors, and platelets (2). Binding of TPO to the c-Mpl receptors in the bone marrow activates intracellular transcriptional pathways leading to an increase in circulating platelet counts (3). Recombinant TPO was effective in stimulating the production of platelets in thrombocytopenic patients in clinical trials (2). However, early forms of recombinant TPO were associated with undesirable immunogenicity where neutralizing antibodies to endogenous TPO were observed (3).

Romiplostim is produced by recombinant DNA technology in Escherichia coli with a molecular weight of 59 kilodaltons. Structurally, romiplostim is an Fc fusion protein (peptibody) that contains two copies of the Fc portion of a human immunoglobulin (IgG_1), each of which is covalently linked to a peptide chain containing two thrombopoietin receptor-binding peptides (TMP) (4,5). It is a novel thrombopoietin mimetic agent with the same mechanism of action as the endogenous TPO (eTPO). As romiplostim has no amino acid sequence homology to eTPO, administration of romiplostim is not expected to elicit immunogenic responses against eTPO. The success in clinical development of romiplostim has resulted in global regulatory approval of romiplostim for the treatment of adults with thrombocytopenia associated with immune thrombocytopenia (ITP). We investigated the pharmacoki-

netics (PK) of romiplostim in rodent species. In this paper, we report the findings from multiple studies with a focus on the clearance mechanism.

MATERIALS AND METHODS

Study Drug

Romiplostim test article and vehicle were manufactured by Amgen Inc. (Thousand Oaks, CA). Dosing solutions were prepared by diluting the romiplostim test article with romiplostim vehicle at appropriate concentrations and volumes to achieve the intended doses.

Animal Experiments

All animal experiments were compliant with the *Guide for the Care and Use of Laboratory Animals*, National Resource Council, National Academy Press, Washington D.C., 1996. Studies were conducted at Amgen Inc., Thousand Oaks, CA according to the study protocols and Amgen's Standard Operating Procedures (SOPs). All animals were acclimated to study rooms for at least 2 days prior to the initiation of the studies and maintained under a 12-hour light and dark cycle. Food and water were given *ad libitum*.

Mice Studies

Normal/wild-type (WT) male mice (C57BL/6 J strain), and FcRn knockout (KO) male mice (special C5BL/6 J-B2m strain), and chemotherapy-induced thrombocytopenic mice, from Jackson Laboratories (Bar Harbor, ME) were used in the studies. The animals weighed around 15–30 g on the first day of dosing.

FcRn Knockout

A single IV bolus dose of romiplostim was administered via the tail vein to 264 FcRn KO mice at 100, 300, or 1000 μg/kg and to 152 WT mice at 100, and 1000 μg/kg. Blood samples were collected for PK evaluation in a composite sampling design where terminal samples were collected from three mice at each time point in each dose group for up to 20 h in FcRn KO mice and up to 96 h in WT mice.

Thrombocytopenia Induced by Chemotherapy and Irradiation

Thrombocytopenia was induced by an intraperitoneal injection of 62.5 mg/kg of carboplatin, reconstituted with 15 mL of 0.9% injectible saline to a stock concentration of 10 mg/mL. Four hours later, mice were exposed to five Grey whole body radiation. Twenty-five WT mice and 35 thrombocytopenic mice were administered a single IV bolus dose of 3 or 30 μg/kg of romiplostim 11 days after the induction of thrombocytopenia. Blood samples were collected for PK evaluation in a composite sampling design where five animals were sampled at each time point for each dose group up to 24 h postdose.

Rat Studies

Male Sprague–Dawley rats (250–350 g) from Charles River Laboratories (Raleigh, NC) were used for the splenectomy study, and male Sprague–Dawley rats (275–375 g) from Hilltop Lab Animals Inc. (Scottdale, PA) were used for the nephrectomy study.

Effect of Splenectomy

Thirty-six rats were anesthetized using 50 mg/kg Nembutal via intraperitoneal injection and supplemented with Metofane as needed to maintain the appropriate level of consciousness. One day prior to dosing, all 36 animals had two silastic cannula surgically inserted, one into the right jugular vein for blood withdrawal and one into the right femoral vein for intravenous dose administration. Control animals ($n=12$) were not involved in any surgical procedures. One day prior to dosing, the spleen was located and removed from 12 rats (splenectomized rats), and the spleen was located and gently manipulated in 12 rats (sham-operated rats). All animals received a single dose of 100 or 1000 μg/kg romiplostim. Blood samples were collected from jugular vein for up to 168 h postdose for PK assessment.

Effect of Nephrectomy

Twenty-four jugular vein pre-cannulated rats were anesthetized. Then, both kidneys were located and removed from eight rats (bilateral nephrectomized rats), and the kidneys were located and gently manipulated in eight rats (sham-operated rats). Control animals ($n=8$) were not involved in any surgical procedures. Within 2 h after the last nephrectomy or sham procedure, all 24 animals received a single IV bolus dose of romiplostim into the femoral vein at 30 or 300 μg/kg ($n=4$/dose group). Blood samples were collected from the jugular vein for up to 12 h postdose.

Evidence of Catabolic Elimination

Eight male animals received a single IV bolus dose of 300 μg/kg romiplostim. PK samples were collected based

on a composite sampling design: 2 animals were sacrificed and sampled at each time point up to 168 h postdose. For each serum sample, a second aliquot was analyzed using anti-TMP/anti-Fc ELISA in addition to the analysis of one aliquot by the primary assay (anti-TMP/anti-TMP ELISA).

Analytical Methods

Quantification of romiplostim in the serum of the rodents was achieved using a basic bridging immunoassay (the primary assay) adapted to form several species/strain-specific analytical methods. The individual methods had the lower limit of quantifications (LLOQs) ranging from 0.270 to 1.77 ng/mL and the upper limit of quantifications (ULOQs) ranging from 10.9 to 46.2 ng/mL. Standards, quality controls (QCs), and test samples containing romiplostim in the serum were allowed to react with a capture antibody (rabbit anti-TMP polyclonal antibody) coated to micro titer wells. After washing away any unbound romiplostim, a detection antibody (biotinylated rabbit polyclonal anti-TMP antibody) was added to the wells to form a bridge. Subsequently, the unbound conjugate was washed away, and horseradish peroxidase (HRP)-labeled streptavidin was added to the wells. Following a final washing step, a substrate solution containing tetramethylbenzidine (TMB) and hydrogen peroxide was added to the wells to produce a colorimetric signal, which was proportional to the amount of romiplostim bound by the capture reagent in the initial step. Color development was stopped using an acid solution, and optical density was measured at 450 nm (OD_{450}). The conversion from OD_{450} units to serum concentrations was achieved using a computer-mediated, log-log or four-parameter regression model fitted to a standard curve.

In one rat experiment, a second bridging immunoassay assay with the same capture antibody and a different detection antibody was utilized. Rat serum samples were allowed to react with the rabbit anti-TMP antibody coated to the microtiter wells. Unbound romiplostim was washed away, and the bound romiplostim was allowed to react with an HRP-labeled mouse anti-human IgG_1 antibody, which served as a detection antibody. After another washing step, a substrate solution containing TMB and hydrogen peroxide was added to the wells. TMB reacted with the peroxide in the presence of HRP and produced a colorimetric signal that was proportional to the amount of romiplostim bound by the capture reagent in the initial step. The color development was stopped and OD_{450} was measured. The conversion of OD_{450} units for the test samples and the QC samples to concentration was achieved through a computer software-mediated comparison to a standard curve on the same run, which was regressed according to a 4-parameter logistic model. The assay had a range of 1.25-50.0 ng/mL.

Accuracy (+/− 15%) and precision (≤20%) were successfully demonstrated using validation samples prepared at five concentrations that span the range of the standard curve including the LLOQ and ULOQ. Some samples required dilution prior to reacting with the capture antibody because they contained concentrations higher than the ULOQ.

Data Analysis

Pharmacokinetic parameters were calculated using standard noncompartmental methods in WinNonlin Professional (Pharsight Inc., Mountain View, California). The concentration at time zero (C_0) was calculated via linear back-extrapolation to time zero using the first two time points. The rate constant of the terminal phase (λ) was calculated via linear regression of the log-linear decay of the terminal phase using at least the last three time points with detectable serum concentrations and was used for extrapolation of the area under the serum concentration-time curve to infinity ($AUC_{0-\infty}$). $AUC_{0-\infty}$ was estimated as the sum of corresponding AUC_{0-t} and C_{last}/λ values where C_{last} was the last measurable concentration. Systemic clearance (CL) was calculated as the dose divided by $AUC_{0-\infty}$. Terminal half-life ($t_{1/2}$) was calculated, when appropriate, as $0.693/\lambda$. The central volume of distribution (V_c) was calculated as $Dose/C_0$. The volume of distribution at steady state (V_{ss}) was calculated as $Dose*AUMC_{0-\infty}/AUC_{0-\infty}^2$ where AUMC is the area under the first moment of the concentration-time curve.

RESULTS

Pharmacokinetics in FcRn Knockout Mice *vs*. Normal (WT) Mice

The involvement of FcRn on the romiplostim disposition was assessed by comparing the romiplostim pharmacokinetic profiles in FcRn KO mice and normal WT mice administered a single IV dose at 100 and 1000 μg/kg (Table I and Fig. 1). The circulating concentration of romiplostim was higher in the normal mice than in the FcRn KO mice at both dose levels. The presence of FcRn resulted in a slower systemic elimination of romiplostim as evidenced by the 16- to 24-fold higher clearance in the FcRn KO mice, suggesting that FcRn serves to protect the degradation or elimination of romiplostim. In both normal and KO mice, the CL, V_c, and V_{ss} values decreased with increasing dose indicating PK nonlinearity. Over the 10-fold dose range (100–1000 μg/kg), the CL values differed by about 2.5-fold (128 *vs.* 318 mL/h/kg) in the FcRn KO mice and about 1.5-fold (8.2 *vs.* 13.1) in the normal mice.

Table I Pharmacokinetic Parameters of Romiplostim in Normal (WT) and FcRn Knockout Mice Following a Single Intravenous Dose

Parameter	Normal		FcRn Knockout		
	$n = 264$		$n = 152$		
Dose (μg/kg)	100	1000	100	300	1000
C_0 (ng/mL)	1570*	26400	485	2630	25400
$AUC_{0-\infty}$ (ng*hr/mL)	10400	146000	427	1980	9380
CL (mL/h/kg)	13.1	8.23	318	212	128
V_c (mL/kg)	86.5	45.6	280	160	47.5
V_{ss} (mL/kg)	104	158	406	464	193

Data represent values rounded to three significant figures.

*Observed concentration value at 0.333 h.

The V_c and V_{ss} values decreased by about 6-fold and 2-fold, respectively, in the knockout mice and 2 fold and 1.5-fold, respectively, in the normal mice. The observed nonlinearity in CL, V_c, and V_{ss} is presumably attributable to the saturation of the binding capacity of the target proteins with increasing romiplostim dose.

Pharmacokinetics in Normal *vs*. Thrombocytopenic Mice

The effect of platelets on the romiplostim pharmacokinetics was assessed at IV doses of 3 and 30 µg/kg in a comparative study of mice with normal platelet counts *versus* mice with thrombocytopenia. The baseline average (SD) platelet counts were 1008.3 $(140.4)\times10^9$/L in normal mice and 144.1 $(54.0)\times10^9$/L in thrombocytopenic mice. Based on the serum concentration profiles over 24 h postdose (Fig. 2), the thrombocytopenic mice had a higher exposure than normal mice at 3 µg/kg, whereas similar exposures were observed in normal and thrombocytopenic mice at 30 µg/kg. This observed dose-dependent impact of platelet counts on serum romiplostim concentrations suggests that the process by which platelets are involved in the romiplostim pharmacokinetics is saturable at high romiplostim dose. Additionally, a 10-fold increase in the romiplostim dose was associated with an approximately similar (13-fold) increase of exposure, assessed by both C_0 and $AUC_{0\text{-}24hr}$, in thrombocytopenic mice. This apparent dose proportionality suggests that the nonlinear process is near or at saturation point for both dose levels when the platelet counts are low. Of note, the exposure at 3 µg/kg dose was not quantifiable in normal mice. Taken together the data suggested that platelets were involved in the romiplostim disposition, likely both distribution and elimination, of romiplostim, and this mechanism can be saturated with increasing romiplostim dose.

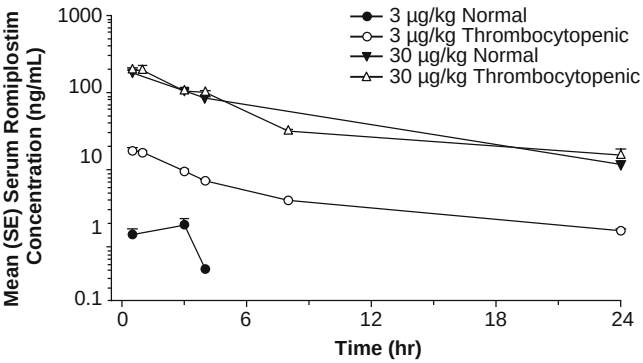

Fig. 2 Pharmacokinetic profile of romiplostim in normal *versus* thrombocytopenic mice following a single IV dose at 3 and 30 μg/kg.

Pharmacokinetics in Control *vs*. Splenectomized Rats

The involvement of the spleen in the disposition of romiplostim was assessed in splenectomized, sham-operated, and control rats administered a single IV dose of 100 or 1000 µg/kg romiplostim. Overall, the romiplostim concentration-time profiles in control, sham-operated, and splenectomized male rats were similar at IV doses of 100 and 1000 µg/kg (Fig. 3). Following an IV dose of romiplostim at 100 and 1000 µg/kg, the sham-operated and

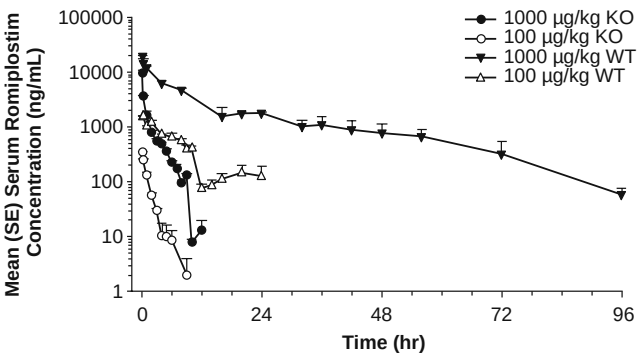

Fig. 1 Pharmacokinetic profile of romiplostim in normal wild-type (WT) and FcRn knockout (KO) mice following a single IV dose at 100 and 1000 μg/kg.

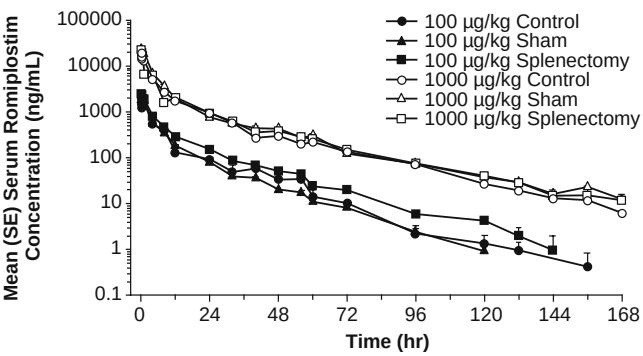

Fig. 3 Pharmacokinetic profile of romiplostim in control, sham-operated, and splenectomized Sprague-Dawley rats following a single IV dose at 100 and 1000 μg/kg.

splenectomized rats had a similar serum romiplostim exposure as the control rats, approximately 0.99- to 1.50-fold for $AUC_{0-\infty}$ and 0.96- to 1.33-fold for C_0. When compared to the sham-operated rats, the splenectomized rats had a slightly higher $AUC_{0-\infty}$ (1.45-fold) and C_0 (1.38-fold) at 100 μg/kg dose and a slightly lower $AUC_{0-\infty}$ (0.76-fold), at 1000 μg/kg dose with similar C_0 (Table II). The lack of a consistent trend at two dose levels suggests that splenectomy does not affect the pharmacokinetics of romiplostim and the observed differences are likely due to variability associated with the surgical procedures. The romiplostim clearance in control rats was similar at 100 and 1000 μg/kg doses, indicating that the romiplostim elimination followed first-order linear kinetics and the associated elimination half-life was approximately 25 h.

Pharmacokinetic Profile of Control *vs*. Nephrectomized Rats

The involvement of the kidney in the disposition of romiplostim was assessed in nephrectomized, sham-operated, and control rats administered IV doses of 30 or 300 μg/kg romiplostim. At 300 μg/kg, nephrectomized rats had 80% higher exposure than control and sham-operated rats; whereas at 30 μg/kg the difference was 26% (Table III and Fig. 4). The results indicate that the kidneys play a major role in the disposition of romiplostim at high dose and the contribution decreases with decreasing romiplostim dose.

Pharmacokinetic Profile of Control Rats: Evidence of Catabolic elimination

In this experiment, the same serum samples were analyzed using two different methods with differing detection antibodies. As shown in the PK profiles (Fig. 5), the romiplostim concentration at the first time point were similar, whereas at the subsequent time points the romiplostim concentrations determined by the anti-TMP/anti-TMP ELISA were consistently lower than those from the anti-TMP/anti-Fc ELISA. This is presumably due to the inability of the anti-TMP/anti-TMP ELISA to measure the catabolically degraded species with less than two TMP peptide chains in serum. The AUC value differed by approximately 3-fold (Table IV), suggesting that the catabolic degradants of romiplostim accounted for about two-thirds of the total circulating species with fragmented TMP bound to Fc.

DISCUSSION

Romiplostim is a recombinant Fc fusion protein product (a peptibody) which was engineered, among other features, 1) to have the Fc domain of the human IgG_1 to interact with the FcRn receptors and 2) to have no sequence homology with TPO in the binding domain for TPO receptor c-Mpl. In particular, these features of romiplostim address issues observed in clinical trials with the predecessor molecule human recombinant megakaryocyte growth and development factor (rhuMGDF), namely a short half-life requiring frequent dosing on a daily basis and the immunogenicity producing antibodies against the eTPO. The clinical development programs of romiplostim confirmed the designed features achieved the intended goals in that romiplostim is approved for weekly dosing and there has been no reported incidence of patients developing antibody against the eTPO. In the preclinical development programs, we conducted several animal studies to evaluate the involvement of FcRn, platelets, spleen, kidneys, and catabolism in the romiplostim clearance and disposition in general.

FcRn, i.e., the Brambell receptor, is known to be involved in the recycling of both the endogenous and exogenous antibody, which in turn contributes to the characteristically long half-life of antibodies. Taking advantage of this natural salvage pathway, scientists utilize the approach of covalent binding of small proteins or peptides to the Fc domain of human immunoglobulins to achieve a prolonged half-life when compared to the naked proteins or peptides. There are several FDA-approved Fc-fusion proteins such as etanercept, alefacept, and abatacept.

Table II Pharmacokinetic Parameters of Romiplostim in Control, Sham-Operated and Splenectomized Sprague-Dawley Rats

	Control		Sham-Operated		Splenectomized	
	n = 12		*n* = 12		*n* = 12	
Dose (μg/kg)	100	1000	100	1000	100	1000
C_0 (ng/mL)	1910	21300	1840	24800	2540	24700
$AUC_{0-\infty}$ (ng*hr/mL)	10700	101000	11100	132000	16100	99900
CL (mL/h/kg)	9.33	9.88	8.98	7.60	6.21	10.0
V_{ss} (mL/kg)	124	153	96.5	113	92.3	185
$t_{1/2}$ (h)	24.9	24.5	15.3	29.9	18.6	25.7

Data represent values rounded to three significant figures.

Table III Pharmacokinetic Parameters of Romiplostim in Control, Sham-Operated and Bilateral Nephrectomized Sprague-Dawley Rats

	Control		Sham-Operated		Nephrectomized	
	n = 8		*n* = 7-8		*n* = 8	
Dose (μg/kg)	30	300	30	300	30	300
C_0 (ng/mL)	492(40)	8350(680)	528(106)	7370(190)	613(87.0)	7040(690)
$AUC_{0\text{-}12hr}$ (ng*hr/mL)	1900(2200)	23800(1900)	1970(260)	22700(1500)	2490(180)	40900(4600)

All values are reported as mean (SD) rounded to three significant figures.

Supporting evidence of the involvement of FcRn in prolonging the half-life of romiplostim was obtained in our mouse study where the single dose romiplostim PK was compared between FcRn KO mice and normal mice. Following a single IV dose, romiplostim was cleared more rapidly in FcRn KO mice compared to in normal mice leading to a lower overall systemic exposure. Comparison of the PK profiles presented in Fig. 1 readily reveal that romiplostim has a prolonged stay in the systemic circulation of WT mice, indicating a longer half-life was achieved due to the presence of FcRn. At 1000 μg/kg dose, the estimated romiplostim half-life in normal mice was 12.5 h, whereas the romiplostim serum concentrations dropped below the limit of quantification within 24 h in the FcRn KO mice. Additionally, the systemic clearance and volume of distribution of romiplostim are both dose dependent, i.e., decrease with increasing romiplostim dose, suggesting target-mediated drug disposition (TMDD) (6). This is also observed in the romiplostim study in healthy human subjects (7).

Multiple lines of evidence, both *in vitro* and *in vivo*, indicated that c-Mpl receptors are involved in the clearance of eTPO. Li *et al.* reported that *in vitro* TPO binding to the receptors on the platelets resulted in internalization of TPO leading to subsequent degradation of TPO (8). An inverse relationship between the platelet counts and the eTPO concentrations has been observed *in vivo* both in animals and in humans (9,10). Two animal studies were conducted to further our understanding of the role of platelets in the dispositon of romiplostim. Chemical and irradiation-induced thrombocytopenic state was generated in mice where the platelet counts were reduced from a normal level of $1008.3(140.4)\times10^9$/L to $144.1(54.0)\times10^9$/L, an approximately 86% reduction in the platelet counts. Thrombocytopenic mice had a higher serum exposure of romiplostim than normal mice at low romiplostim dose but a similar exposure to the nomal mice at high romiplostim dose. This is consistent with the saturable nature of the c-Mpl receptors due to its capacity limit which appeared to be saturated at a dose of 30 μg/kg and higher. Because the c-Mpl receptors are the pharmacological target of romiplostim and involved in the disposition, both distribution and elimination, romiplostim PK therefore involves TMDD. It is well known that the c-Mpl receptors are also expressed on the megakaryocytes, the precursor cells residing in the bone marrow (3,11). Chemotherapy and irradiation causes pancytopenia in the bone marrow leading to a reduced pool of the precursor cells of platelet in addition to the reduction in the circulating platelet counts. Consequently, the overall impact of this combination treatment on the target pool may be greater than measured by the circulating platelet counts.

Surgical removal of the spleen in rats is another model that reflects a state of reduced overall systemic

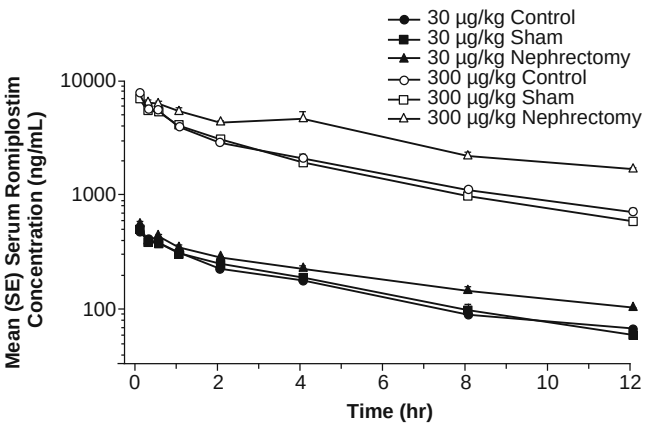

Fig. 4 Pharmacokinetic profile of romiplostim in control, sham-operated, and nephrectomized Sprague-Dawley rats following a single IV dose at 30 and 300 μg/kg.

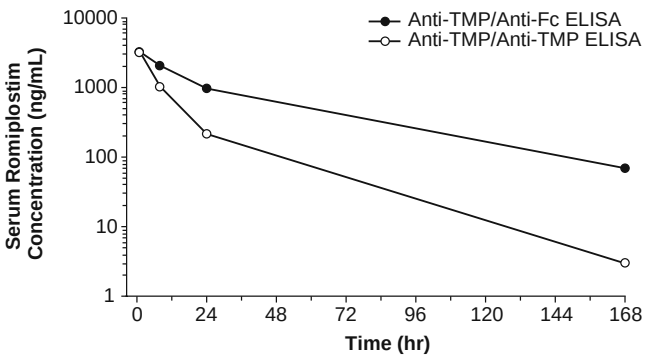

Fig. 5 Pharmacokinetic profile of romiplostim in male Spague-Dawley rats following a single IV dose at 300 μg/kg.

Table IV Pharmacokinetic Parameters of Romiplostim Derived from Two Different ELISA Assays in Rats Administered a Single IV Bolus Dose at 300 μg/kg

	Anti-TMP/Anti-TMP ELISA $n = 2$/timepoint	Anti-TMP/Anti-Fc ELISA $n = 2$/timepoint
C_0 (ng/mL)	3730	3450
$AUC_{0-168hr}$ (ng*hr/mL)	43300	120000

Data represent values rounded to three significant figures.

platelet counts because the spleen is a known reservoir for platelets that are sequestered from systemic circulation (12,13). Under normal physiological conditions, the spleen sequesters one-third of the platelets which are released into circulation at times of vascular stress. Provided that all the platelets sequestered in the spleen were removed by the sugical procedure, the rats would have had a 33% reduction in the platelet counts. It is not unlikely though the surgical operation presented a condition in which the spleen released the sequestered platelet for emergency use. If this were the case, the extent of circulating platelet count reduction would be smaller than 33%. In addition, the overall pool of c-Mpl extends beyond the systemic circulation and includes the precursor cells in the bone barrow. Taken together, it is not unreasonable that the effect of platelets on romiplostim PK was observed readily in the chemotherapy/irradiation-induced thrombocytopenic mice model but not in the splenectomized rat model.

Both small molecule pharmaceuticals and protein therapeutics are typically broken down enzymatically before they are eliminated from the systemic circulation. While cytochrome P450 enzymes are commonly involved in the metabolic degradation of small molecule pharmaceuticals, they do not contribute to the breakdown of protein therapeutics. Instead, the catabolic breakdown of protein therapeutics involves the same enzymes that catabolize proteins in food intake. The romiplostim experiment revealed indirect evidence that circulating breakdown product(s) of romiplostim existed in rats and suggested the peptide portion of the molecule was more susceptible to catabolism than the Fc portion. The catabolic pathway plays an important role in the systemic clearance of romiplostim, with catabolic degradants accounting for about 60% of the overall total circulating species related to romiplostim molecules. To study the biotransformation and investigate the structure of the circulating breakdown product, follow-up *in vivo* experiments were conducted in rats and the ligand-binding mass spectrometry method was utilized for structural elucidation (4). Collectively, the data support the notion that covalent binding of thrombopoietin mimetic peptides to Fc domain of the human gamma immunoglobulin increases the overall stability of the peptides and prolonged the systemic residence time of the peptides, consistent with the molecular design goal for romiplostim.

The kidney is commonly involved in the elimination of therapeutic agents. However, the renal elimination of macromolecules is subject to the limitations of the molecular weight and the conformation, among other factors (14). Small proteins such as insulin, human growth hormone, and antibody Fab fragments are excreted in the urine (15–17). Catabolic breakdown of large protein molecules, either systemically or locally in kidney tissues, often precedes urinary excretion (15,18,19). Thus, the characterization of the extent of renal excretion of protein therapeutics is not commonly done. In our experiment, romiplostim serum concentrations were monitored over 12 h post-dose in nephrectomized rats. This study duration reflected the viability constraints of the surgical animal model. Nephrectomy in rats resulted in a decrease in overall romiplostim clearance, and higher romiplostim exposure indicates that the renal elimination pathway plays a role in the romiplostim disposition. The contribution of the kidney to romiplostim elimination increases with increasing romiplostim dose. This observed dose-dependent renal contribution is most likely due to the nonlinearity in the competing elimination mechanism such as binding to the c-Mpl receptors (discussed above), because glomerular filtration is commonly known as a linear process with a constant elimination rate, i.e., independent of the administered dose. At low dose the circulating romiplostim concentration is low, and binding to the target c-Mpl receptors represents the major elimination pathway due to high affinity molecular interactions. With increasing dose, receptor binding capacity gradually approaches saturation; hence, the contribution of target-mediated pathway to the overall elimination of romiplostim diminishes with increasing dose. Urinary excretion then becomes a more prominent elimination route as romiplostim dose increases. Consequently, we anticipate the kidneys to have small contributions to romiplostim elimination in the clinical setting as the maximum recommended clinical dose (10 μg/kg) is lower than 30 μg/kg, where rats showed 26% increase in AUC_{0-12hr}, and the target-mediated elimination pathway is expected to be greater. The relative contributions of the linear and nonlinear elimination routes were explored based on a PK/PD model of romiplostim in healthy human subjects (20).

CONCLUSIONS

Both endogenous thrombopoietin and recombinant thrombopoietin have short half-lives. Romiplostim has the same

mechanism of action and was engineered to have improved pharmacokinetic properties. Our pharmacokinetic studies in rodents revealed the romiplostim clearance involved multiple mechanisms, including catabolism, renal excretion, and binding to target receptors on platelets. The target receptor-mediated mechanism is saturable, and the relative contribution of different mechanisms appear dose-dependent. Such mechanistic understanding in rodents laid the foundation for the study of romiplostim pharmacokinetics in humans.

ACKNOWLEDGMENTS

A portion of the reported data was presented at the 2005 ASH Annual Meeting as a poster presentation by Yu-Nien Sun, Rosalin Arends, Anthony Smithson, Ann Watson, and Janet L. Nichol. A Novel Thrombopoiesis-Stimulating Agent, AMG 531: Pharmacokinetics and Pharmacodynamics in FcRn Knock-Out and Wild Type Mice. Published in Blood (ASH Annual Meeting Abstracts), Nov 2005; 106: 3575. The authors of this manuscript (Yow-Ming C Wang, Bethlyn Sloey, Teresa Wong, Prerna Khandelwal, Rebeca Melara, and Yu-Nien Sun), are employees of Amgen Inc., which supported this study. The authors wish to thank Michelle Zakson for editing/writing assistance. We greatly appreciate the contribution of a broader Amgen team that worked on the development program of romiplostim over more than a decade of time. The team members, listed in alphabetical order, include, but are not limited to, the following: Rosalin Arends, Sharon Baughman, Beckinam Cepeda, Binodh de Silva, Lena Henday, Jessica Johnson, Janet Nichol, Jose Rodriquez, Anthony Smithson, Bing Wang, Tian Wang, Jeana Warren, Ann Watson, Lynn Wetherwax, Bing-Bing Yang and Protein Labs at Amgen PKDM.

REFERENCES

1. Cohen-Solal K, Debili N, Vainchenker W, Wendling F. Thrombopoietin (Mpl-ligand) and the regulation of platelet production. Thromb Haemost. 1997;78:37–41.
2. Brown AS EJ, Martin JF. Megakaryocytopoiesis: the megakaryocyte/platelet haemostatic axis. In: Franz von Bruchhausen UW, editor. Platelets and Their Factors: Springer; 1 edition (July 15, 1997) 1997. p. 3–26.
3. Jackson C, Arnold JT, Pestina TI, Stenberg PE. Megakaryocyte Biology. In: Kuter DJ, Hunt P, Sheridan W, Zucker-Franklin D, editors. Thromobopoiesis and Thrombopoietins; Molecular, Cellular, Preclinical, and Clinical Biology. Totowa, New Jersey.: Humana Press; 1997. p. 3–40.
4. Hall MP, Gegg C, Walker K, Spahr C, Ortiz R, Patel V, *et al.* Ligand-Binding Mass Spectrometry to Study Biotransformation of Fusion Protein Drugs and Guide Immunoassay Development: Strategic Approach and Application to Peptibodies Targeting the Thrombopoietin Receptor. AAPS J.
5. Molineux G, Newland A. Development of romiplostim for the treatment of patients with chronic immune thrombocytopenia: from bench to bedside. Br J Haematol. 2010;150:9–20.
6. Mager DE, Jusko WJ. General pharmacokinetic model for drugs exhibiting target-mediated drug disposition. J Pharmacokinet Pharmacodyn. 2001;28:507–32.
7. Wang B, Nichol JL, Sullivan JT. Pharmacodynamics and pharmacokinetics of AMG 531, a novel thrombopoietin receptor ligand. Clin Pharmacol Ther. 2004;76:628–38.
8. Li J, Xia Y, Kuter DJ. Interaction of thrombopoietin with the platelet c-mpl receptor in plasma: binding, internalization, stability and pharmacokinetics. Br J Haematol. 1999;106:345–56.
9. Kuter DJ, Rosenberg RD. The reciprocal relationship of thrombopoietin (c-Mpl ligand) to changes in the platelet mass during busulfan-induced thrombocytopenia in the rabbit. Blood. 1995;85:2720–30.
10. Engel C, Loeffler M, Franke H, Schmitz S. Endogenous thrombopoietin serum levels during multicycle chemotherapy. Br J Haematol. 1999;105:832–8.
11. Geddis AE, Linden HM, Kaushansky K. Thrombopoietin: a pan-hematopoietic cytokine. Cytokine Growth Factor Rev. 2002;13:61–73.
12. Hoffbrand AV. Oral iron chelators in the treatment of hematologic diseases. Clin Adv Hematol Oncol. 2005;3:536–8.
13. Stoelting RK, Miller Ronald D. Basics of anesthesia 5th ed. Churchill Livingstone: Elsevier; 2007. p. 338.
14. Chen B, Jerger K, Frechet JM, Szoka Jr FC. The influence of polymer topology on pharmacokinetics: differences between cyclic and linear PEGylated poly(acrylic acid) comb polymers. J Control Release. 2009;140:203–9.
15. Hansen CP, Goetze JP, Stadil F, Rehfeld JF. Excretion of progastrin products in human urine. Am J Physiol. 1999;276:G985–92.
16. Ujhelyi MR, Robert S. Pharmacokinetic aspects of digoxin-specific Fab therapy in the management of digitalis toxicity. Clin Pharmacokinet. 1995;28:483–93.
17. Proksch JW, Gentry WB, Owens SM. Pharmacokinetic mechanisms for obtaining high renal coelimination of phencyclidine and a monoclonal antiphencyclidine antigen-binding fragment of immunoglobulin G in the rat. J Pharmacol Exp Ther. 1998;287:616–24.
18. Behr T, Becker W, Hannappel E, Goldenberg DM, Wolf F. Targeting of liver metastases of colorectal cancer with IgG, F(ab')2, and Fab' anti-carcinoembryonic antigen antibodies labeled with 99mTc: the role of metabolism and kinetics. Cancer Res. 1995;55:5777s–85s.
19. McQuarrie SA, Baum RP, Niesen A, Madiyalakan R, Korz W, Sykes TR, *et al.* Pharmacokinetics and radiation dosimetry of 99Tcm-labelled monoclonal antibody B43.13 in ovarian cancer patients. Nucl Med Commun. 1997;18:878–86.
20. Wang YM, Krzyzanski W, Doshi S, Xiao JJ, Perez-Ruixo JJ, Chow AT. Pharmacodynamics-Mediated Drug Disposition (PDMDD) and Precursor Pool Lifespan Model for Single Dose of Romiplostim in Healthy Subjects. AAPS J.